An agent-based model to examine neuroinvasion by SARS-CoV-2

Varsha Bhat
PES university https://orcid.org/0000-0002-1462-1591
Aditi Lakshmi S
PES University
Abhinaya Muraly
PES University
Pranathi Rao
PES University
Jhinuk Chatterjee (jhinukchatterjee@pes.edu)
PES University https://orcid.org/0000-0003-1193-5488

Short Report

Keywords: Anosmia, neuroinvasion, sustentacular cells, NetLogo 3D

Posted Date: February 9th, 2022

DOI: https://doi.org/10.21203/rs.3.rs-1333474/v1

Abstract

SARS-CoV-2 is known to primarily cause mild to severe respiratory infections as well as chemosensory disturbances such as anosmia. Furthermore, it has been associated with the occurrence of neurological symptoms. In this study probable route of neuroinvasion by SARS-CoV-2 from the olfactory epithelium to the central nervous system was suggested and an agent-based model has been developed using NetLogo 3D. A series of simulations were performed to analyze real-world infection patterns; based on these simulations, it was observed that there is a direct correlation between the age of the patient and the day of neuroinvasion onset.

Introduction

The novel coronavirus strain severe acute respiratory syndrome-coronavirus-2 (SARS-CoV-2) was first discovered in Wuhan, China in early December 2019 [1, 2, 3]. One of the first and most common symptoms exhibited by infected individuals is anosmia: a partial or total loss of smell [4]. Although several theories have been proposed to explain the cause of anosmia, the most probable amongst them is that an infection of sustentacular cells (support cells found in the olfactory epithelium) [4, 5]. Numerous patients infected with SARS-CoV-2 have also displayed neurological symptoms, implying an invasion of the central nervous system (CNS) through the olfactory system [6]. The primary method by which the virus passes to the CNS and then propagates through the CNS needs to be explored more. In this study, a probable route by which SARS-CoV-2 travels from the olfactory epithelium to the brain was suggested and onset of neuroinvasion by SARS-CoV-2 with an agent-based model developed and simulated using NetLogo 3D. Simulations were run for two conditions- patient age greater than 60 years and lesser than 60 years for viral loads 10^3, 10^4 and 10^5.

Methods

Key Concepts

SARS-CoV-2 particles infect an individual mainly through olfactory systems. Support cells in the olfactory tissue, called sustentacular cells, have ACE2 receptors, which provide a gateway through which viral particles can enter, hijack cellular machinery to produce more viral particles, lyse sustentacular cell and infect more cells in the vicinity. Death of these sustentacular cells upends the machinery powering olfactory sensory neurons (OSNs) [7]. Upon cell lysis, a certain number of viral particles enter into either the blood or the lymph. Increase in the permeability of the blood-brain barrier (BBB) by upregulation of IL-6 as well as enlargement of perivascular spaces (PVS) suggest that the SARS-CoV-2 virus might disseminate through the CNS [8,9,6]. Frontal lobe, temporal lobe, cerebellum, corpus callosum and thalamus is most liable to neural cell atrophy.

Model Building

The model was built using NetLogo 3D (version 6.2.0), which facilitates the three-dimensional representation of the system of interest [10]. The system has been divided into three distinct regions: the olfactory epithelium, circulatory system (the heart and the lungs), and the CNS), as seen in Figure 1. Steps are showcased within the NetLogo universe as a series of colorful blocks of varying sizes and shapes. Some blocks represent tissue, while others represent cells. Every effort to maintain a reasonable size ratio has been expended. In the model, the virus passes through the mucus barrier, travels through the olfactory epithelium and the circulatory system, moves past the blood-brain barrier to eventually reach the brain. The infection of the sustentacular cells and the atrophy of the cerebral regions have been depicted in order to represent the phenomena of anosmia as well as neuroinvasion by SARS-CoV-2.

Model Environment

The model was created on a rectangular coordinate system called the NetLogo world, and the x,y and z coordinates were set to -40 to +40, -30 to +30, and -20 to +20, respectively. However, the patches and frames were kept at their default settings of 13 pixels and 30 frames per second respectively. Each organ within the world was constructed with a distinct color to differentiate between systems. Further, the cells, represented as turtles were given different shapes to better visualize interactions and changes if any.

Model Assumptions and Rules

The model assumptions were first declared to design a plausible system and a corresponding model rule to simulate the same. These assumptions and rules were:

- The SARS-CoV-2 virus enters through the nose only. This assumption is to fit the model to the hypothesis that the neuroinvasion of the virus follows anosmia. The virus' first entry point is thus, through the nasal cavity and into the olfactory epithelium after crossing the mucosal barrier.

- The mucus and blood brain barriers do not pose a physical resistance to the movement of the virus. The barriers' effectivity and rate of clearance have not been established in the literature. The barriers are depicted by patches as a visual barrier only.

- The virus can infect only the sustentacular cells within the olfactory epithelium. Only the sustentacular cells possess the necessary entry molecules. When the distance between the virus and the sustentacular cells is less than 0.6, the virus attacks the sustentacular cells.

- From Bar-On et al [11], the virus burst size is approximately 1000. The burst size is appropriately scaled down during the simulation.

- The virus moves along the hematogenous route. The most convenient path for the virus' movement to the central nervous system is through the bloodstream and not the olfactory bulb. This is because of the lack of a gateway molecule in the olfactory sensory neuron, in particular, the ACE2 receptors and primer protease TMPRSS2. The virus invades the lymphatic system from the sustentacular cells. The

virus is then drained along with the lymph into the bloodstream. Through the bloodstream, it is then able to enter the heart and circulates through the system till it finally reaches the blood-brain barrier.

● Cells of a certain type are uniform in shape and size and the role of cilia and microvilli can be performed by the cell surface. The size of the cells varies and is therefore approximated to a uniform value (see Table 1).

● The immune system mounts a response 5 days after symptom onset. The approximate response by the immune system occurs 5 days after symptom onset. After 100 ticks (20 ticks = 1 day), 0-2 viruses are killed in each tick.

● The rate of immune response is lower in individuals aged 60 years and above. The number of viruses killed per tick is relatively lower.

Model Timescales, Variables, and Scaling-down

The values for the sizes and the counts of the model variables were obtained through literature mining; when specific data were not available, estimates based on present knowledge were utilized. As directly implementing the sizes and counts can result in the consumption of a large amount of computational time and resources, they were appropriately scaled down in the model environment so as to reflect realistic infection patterns. The sizes of the variables were scaled in terms of the relative ratios. For example, $\frac{virussize}{sustentacularcellsize} = \frac{0.1}{3}$. For scaling the counts, three mathematical functions were applied:

● For variables in the olfactory epithelium: log(count) * 10

● For variables in the brain: log(count) * 5

● For SARS-CoV-2: $x^{1/3}$

Table 1 lists the sizes and counts of the variables [12–19]. The simulations were performed by changing the viral load using the slider and switching between different attributes (such as the age of the patient) using the choosers on the NetLogo interface. The results were analyzed by tracking the count of the sustentacular cells and brain atrophy via monitors on the interface, along with the number of ticks completed.

Visualization

In order to visualize the data, the viral count at the end of every tick was reported as output from NetLogo 3D; this was then plotted against the corresponding tick value. The plots this generated would help to generalize the trend of the virus' count following infection over time. The plots were categorized according to the age group and further divided based on the initial viral load, resulting in six scenarios.

Table 1
Model Variables

Variable	Size (μm)	Count	Scaled Down Count
SARS-CoV-2	0.1	10^5 copies/mL	10-50
Sustentacular cells	3 - 5	3.33×10^6	65
Olfactory sensory neurons	3 - 5	10^7	70
Frontal lobe neurons	3 - 5	6.56×10^9	49
Temporal lobe neurons	3 - 5	3.52×10^9	48
Cerebellum neurons	3 - 5	69×10^9	54
Corpus callosum neurons	3 - 5	-	46
Thalamus neurons	3 - 5	-	43

Results & Discussion

NetLogo 3D helps provide a 3-dimensional visualization of the dynamic system, making it simpler to comprehend. The inclusion of time and spatial interactions to govern the model allows the accurate simulation of real-life conditions. The relationship between the age of the patient and the day of neuroinvasion onset was examined for three distinct values of viral loads. The simulations were run for two conditions- patient age greater than 60 years and lesser than 60 years for viral loads 10^3, 10^4 and 10^5. For the viral loads of 10^3 (set to 10 on the NetLogo slider), 100 replicate simulations were run for the two scenarios “less than 60 years of age” and “greater than 60 years of age”. The number of ticks at which atrophy in the brain (neuroinvasion) occurred was noted for each replicate, and these values were subsequently converted to the corresponding number of days. The mean number of days for each of the two scenarios was calculated, and the two means were compared with a Welch Two Sample t-test with a significance level of 0.05. The procedure was repeated for the viral loads 10^4 (set to 22 on the NetLogo slider) and 10^5 (set to 46 on the NetLogo slider). The p-values for the three viral loads 10^3,10^4, and 10^5 were 0.0004475, 0.04124, and 0.006138, respectively, indicating a statistically significant relationship between the patient age and day of neuroinvasion onset. This emphasizes the need for increased measures in diagnosing and treating neurological conditions arising in COVID-19 patients, especially the vulnerable population above 60 years of age.

Line graphs generated for the six conditions with varying viral load — 10^4, 10^5, 10^6, and age groups — above and below 60 years of age, help further the preliminary analysis performed by the model. For populations above the age of 60, the viral load peaks around tick 100, and continues to average at the same virus count upto the beginning of neuroinvasion irrespective of the time elapsed. On the other hand, for the population under 60, the virus count gradually declines over time after reaching the peak load upto

the day of onset of neuroinvasion. The trends mentioned here are seen in all three viral load conditions for both age groups. Interestingly, the virus count drops steadily after day 5 for individuals aged less than 60 years; however, the drop is relatively lower for individuals aged 60 years and above. This preliminary analysis yields the result that viral load does not decrease as quickly in the older population when compared to patients under 60. This supports the result of model simulations that the age of the patient is significant with respect to the day of onset of neuroinvasion.The complete results of the simulations are listed in Supplementary Table 1. Figures 2 & 3 depict the relationship between the virus count and time for all the three viral loads and two scenarios.

Conclusion

An agent-based model using NetLogo 3D was developed. Upon running simulations using the model, it was determined that the patient's age is significant with respect to the date of onset of neurological symptoms. The graphs generated for various conditions, built upon the simulation results by showing the downward trend in virus count with time in the condition below 60 years of age, while there was no drastic change of virus count with time seen in the condition above 60 years of age.

The model serves as a preliminary attempt to understand the relatively unexplored area of neuroinvasion in COVID-19. Assumptions used to construct the model may not exhibit all the characteristics and elements of a complex biological system. The model includes only those cells and organs directly interacting with the virus to simplify the system. The data necessary to improve the given model include research into the interaction between the lymphatic system and the virus, high-quality brain MRIs from patients to validate the model, and an exhaustive insight into the different modes of progression of SARS-CoV-2 inside the brain. As the availability of COVID-19 -related data increases, this model can be expanded accordingly to include more variables and simulations in the future. Therefore, this information can guide experimental research, treatment options, and hypothesis testing by researchers and clinical practitioners.

Declarations

Conflict of interest:

The authors declare no conflict of interest.

Funding:

There was no funding source pertaining to this research work.

References

1. Cascella M, Rajnik M, Aleem A, Dulebohn S. C., Napoli R.D. Features, Evaluation, and Treatment of Coronavirus (COVID-19) [Updated 2021 Sep 2]. In: StatPearls [Internet]. Treasure Island (FL):

StatPearls Publishing; 2021 Jan-. Available from: https://www.ncbi.nlm.nih.gov/books/NBK554776/

2. Dong, E., Du, H., & Gardner, L.An interactive web-based dashboard to track COVID-19 in real time. The Lancet. Infectious diseases 2020;20(5):533–534. https://doi.org/10.1016/S1473-3099(20)30120-1
3. Rothan, H. A., & Byrareddy, S. N. The epidemiology and pathogenesis of coronavirus disease (COVID-19) outbreak. Journal of autoimmunity 2020;109: 102433. https://doi.org/10.1016/j.jaut.2020.102433
4. Butowt, R., & von Bartheld, C. S. Anosmia in COVID-19: Underlying Mechanisms and Assessment of an Olfactory Route to Brain Infection. The Neuroscientist: a review journal bringing neurobiology, neurology and psychiatry 2021; 27(6): 582–603. https://doi.org/10.1177/1073858420956905
5. Bryche, B., St Albin, A., Murri, S., Lacôte, S., Pulido, C., Ar Gouilh, M., Lesellier, S., Servat, A., Wasniewski, M., Picard-Meyer, E., Monchatre-Leroy, E., Volmer, R., Rampin, O., Le Goffic, R., Marianneau, P., & Meunier, N. Massive transient damage of the olfactory epithelium associated with infection of sustentacular cells by SARS-CoV-2 in golden Syrian hamsters. Brain, behavior, and immunity 2020; 89: 579–586. https://doi.org/10.1016/j.bbi.2020.06.032
6. Netland, J., Meyerholz, D. K., Moore, S., Cassell, M., & Perlman, S. Severe acute respiratory syndrome coronavirus infection causes neuronal death in the absence of encephalitis in mice transgenic for human ACE2. Journal of virology 2008; 82(15): 7264–7275. https://doi.org/10.1128/JVI.00737-08
7. Villar, P. S., Delgado, R., Vergara, C., Reyes, J. G., & Bacigalupo, J. Energy Requirements of Odor Transduction in the Chemosensory Cilia of Olfactory Sensory Neurons Rely on Oxidative Phosphorylation and Glycolytic Processing of Extracellular Glucose. The Journal of neuroscience: the official journal of the Society for Neuroscience 2017; 37(23):5736–5743.https://doi.org/10.1523/JNEUROSCI.2640-16.2017
8. Zhang, J., Sadowska, G. B., Chen, X., Park, S. Y., Kim, J. E., Bodge, C. A., Cummings, E., Lim, Y. P., Makeyev, O., Besio, W. G., Gaitanis, J., Banks, W. A., & Stonestreet, B. S. Anti-IL-6 neutralizing antibody modulates blood-brain barrier function in the ovine fetus. FASEB journal: official publication of the Federation of American Societies for Experimental Biology 2015; 29(5):1739–1753. https://doi.org/10.1096/fj.14-258822
9. Miyata, M., Kakeda, S., Iwata, S., Nakayamada, S., Ide, S., Watanabe, K., Moriya, J., Tanaka, Y., & Korogi, Y. Enlarged perivascular spaces are associated with the disease activity in systemic lupus erythematosus. Scientific reports 2017; 7(1): 12566. https://doi.org/10.1038/s41598-017-12966-4
10. Wilensky U. NetLogo: Agent-Based Modelling Software. Version 6.2.0 [software]. Northwestern University. 1999.
11. Bar-On, Y. M., Flamholz, A., Phillips, R., & Milo, R. SARS-CoV-2 (COVID-19) by the numbers. eLife 2020; 9: e57309.https://doi.org/10.7554/eLife.57309
12. Pan, Y., Zhang, D., Yang, P., Poon, L., & Wang, Q. Viral load of SARS-CoV-2 in clinical samples. The Lancet. Infectious diseases 2020; 20(4): 411–412. https://doi.org/10.1016/S1473-3099(20)30113-4
13. Helwany M, Bordoni B. Neuroanatomy, Cranial Nerve 1 (Olfactory) [Updated 2021 Aug 11]. In: StatPearls [Internet]. Treasure Island (FL): StatPearls Publishing; 2021 Jan-. Available from:

https://www.ncbi.nlm.nih.gov/books/NBK556051/

14. Klopfenstein, T., Kadiane-Oussou, N. J., Toko, L., Royer, P. Y., Lepiller, Q., Gendrin, V., & Zayet, S. Features of anosmia in COVID-19. Medecine et maladies infectieuses 2020; 50(5): 436–439. https://doi.org/10.1016/j.medmal.2020.04.006
15. Klopfenstein, T., Zahra, H., Kadiane-Oussou, N. J., Lepiller, Q., Royer, P. Y., Toko, L., Gendrin, V., & Zayet, S. New loss of smell and taste: Uncommon symptoms in COVID-19 patients on Nord Franche-Comte cluster, France. International journal of infectious diseases: IJID: official publication of the International Society for Infectious Diseases 2020; 100: 117–122. https://doi.org/10.1016/j.ijid.2020.08.012
16. Herculano-Houzel S. The human brain in numbers: a linearly scaled-up primate brain. Frontiers in human neuroscience 2009; 3: 31. https://doi.org/10.3389/neuro.09.031.2009
17. Liewald, D., Miller, R., Logothetis, N., Wagner, H. J., & Schüz, A. Distribution of axon diameters in cortical white matter: an electron-microscopic study on three human brains and a macaque. Biological cybernetics 2014; 108(5): 541–557. https://doi.org/10.1007/s00422-014-0626-2
18. Kennedy, D. N., Lange, N., Makris, N., Bates, J., Meyer, J., & Caviness, V. S., Jr. Gyri of the human neocortex: an MRI-based analysis of volume and variance. Cerebral cortex 1998; 8(4): 372–384. https://doi.org/10.1093/cercor/8.4.372
19. Cheng, Q., Yang, Y., & Gao, J. Infectivity of human coronavirus in the brain. EBioMedicine 2020; *56*: 102799. https://doi.org/10.1016/j.ebiom.2020.102799

Figures

Figure 1

NetLogo World: Model legend, including the modes of representation of the agents and barriers (SARS-CoV-2: small white spheres; sustentacular cells: light yellow spheres; olfactory sensory neurons: cyan spheres; frontal lobe neurons: blue spheres; temporal lobe neurons: yellow cones; cerebellum neurons: magenta targets)

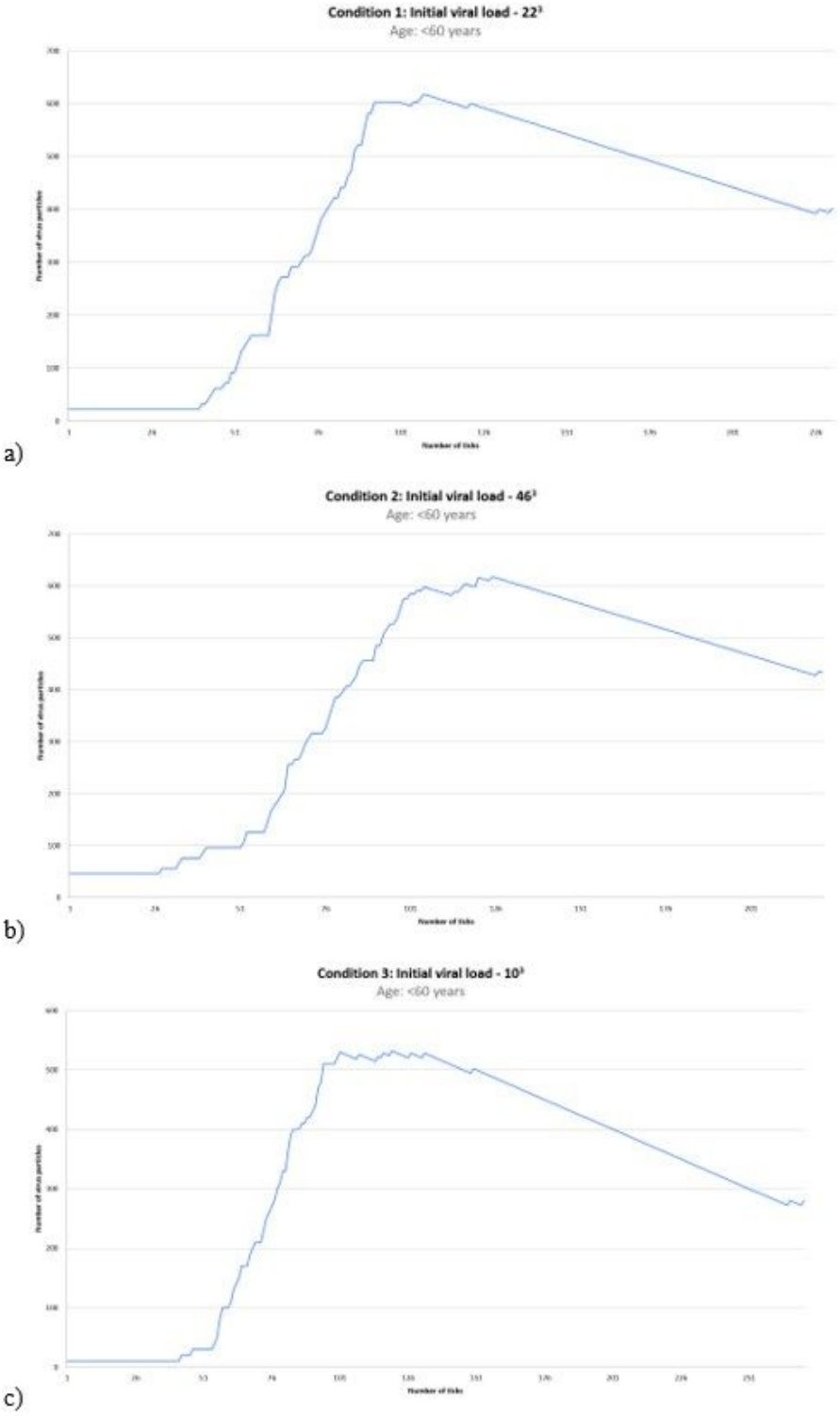

Figure 2

Plot of virus count versus the number of ticks for patients less than 60 years old. a) Initial viral load = 22^3. b) Initial viral load = 46^3. c) Initial viral load = 10^3.

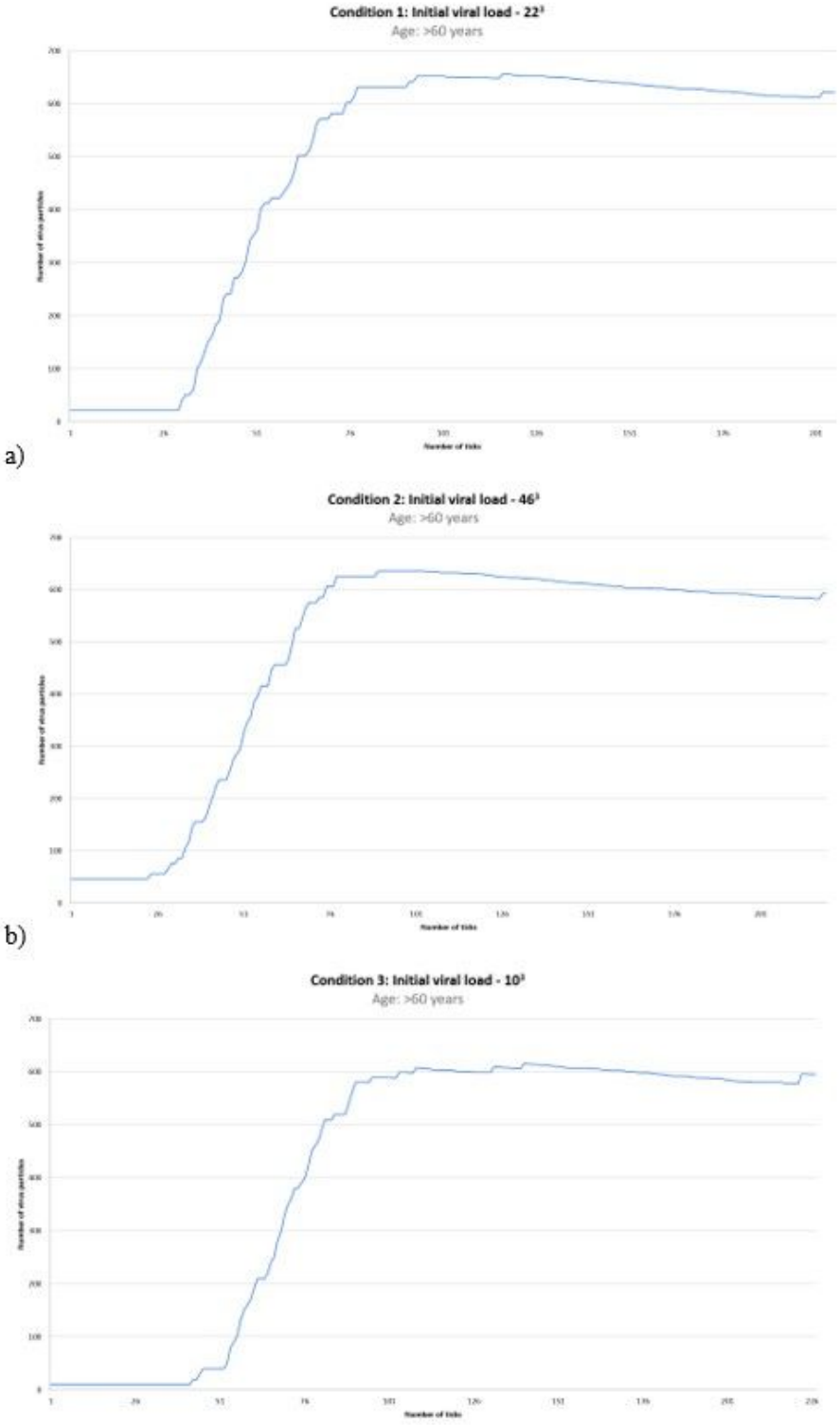

Figure 3

Plot of virus count versus the number of ticks for patients greater than 60 years old. a) Initial viral load = 22^3. b) Initial viral load = 46^3. c) Initial viral load = 10^3.

Supplementary Files

This is a list of supplementary files associated with this preprint. Click to download.

- SupplementaryTableS1.xlsx